Molecular Pharmacology Fast Forward. Published on July 5, 2016 as DOI: 10.1124/mol.116.103416
This article has not been copyedited and formatted. The final version may differ from this version.

TITLE PAGE

Hybrid Enzalutamide Derivatives with Histone Deacetylase Inhibitor Activity Decrease HSP90 and the Androgen Receptor Levels and Inhibit Viability in Enzalutamide Resistant C4-2 Prostate Cancer Cells

Rayna Rosati, Bailing Chen, Mugdha Patki, Thomas McFall, Siyu Ou, Elisabeth Heath, Manohar Ratnam and Zhihui Qin

RR, MP, TM, EH, MR: Barbara Ann Karmanos Cancer Institute and Department of Oncology, Wayne State University, Detroit, MI 48201-2013

BC, SO, ZQ: Department of Pharmaceutical Sciences, Wayne State University, Detroit, MI 48201-2013

Molecular Pharmacology Fast Forward. Published on July 5, 2016 as DOI: 10.1124/mol.116.103416
This article has not been copyedited and formatted. The final version may differ from this version.

RUNNING TITLE PAGE

Running Title: Enzalutamide-histone deacetylase inhibitor hybrid molecules

Corresponding author: Manohar Ratnam, Ph.D., 4100 John R, HWCRC 840.1, Detroit, MI 48201. Tel: 313-576-8612. Email: ratnamm@karmanos.org

Number of text pages: 37

Tables: 0

Figures: 9

References: 70

# of words in Abstract: 249

# of words in Introduction: 992

# of words in Discussion: 1107

Non-standard abbreviations; Enz, Enzalutamide; SAHA, Suberoylanilide hydroxamic acid; HDAC, Histone deacetylase; HDACi, Histone deacetylase inhibitor; PCa, Prostate cancer; CRPC, Castration recurrent prostate cancer; AR, Androgen receptor

Molecular Pharmacology Fast Forward. Published on July 5, 2016 as DOI: 10.1124/mol.116.103416
This article has not been copyedited and formatted. The final version may differ from this version.

Abstract

Histone deacetylase (HDAC) inhibitors (HDACi) can disrupt viability of prostate cancer (PCa) cells through modulation of the cytosolic androgen receptor (AR) chaperone protein HSP90. However, toxicities associated with their pleiotropic effects could contribute to the ineffectiveness of HDACi in PCa treatment. We designed hybrid molecules containing partial chemical scaffolds of enzalutamide and suberoylanilide hydroxamic acid (SAHA), with weakened intrinsic pan-HDACi activities, to target HSP90 and AR in enzalutamide-resistant PCa cells. The potency of the new molecules (**2-75** and **1005**) as inhibitors of nuclear and cytosolic HDACs was substantially lower than that of SAHA in cell-free and *in situ* assays. **2-75** and **1005** antagonized gene activation by androgen without inducing chromatin association of AR. Enzalutamide had no effect on the levels of AR or HSP90 whereas the hybrid compounds induced degradation of both AR and HSP90, similar to (**1005**) or more potently than (**2-75**) SAHA. Similar to SAHA, **2-75** and **1005** decreased the level of HSP90 and induced acetylation in a predicted ~55 KDa HSP90 fragment. Compared to SAHA, **2-75** induced greater hyper-acetylation of the HDAC6 substrate alpha-tubulin but in contrast to SAHA neither hybrid molecule caused substantial hyper-acetylation of histones H3 and H4. **2-75** and **1005** induced p21 and caused loss of viability in the enzalutamide-resistant C4-2 cells with efficacies that were comparable to or better than SAHA. The results suggest the potential of the new compounds as prototype antitumor drugs that would downregulate HSP90 and AR in enzalutamide-resistant prostate cancer cells with weakened effects on nuclear HDACi targets.

Molecular Pharmacology Fast Forward. Published on July 5, 2016 as DOI: 10.1124/mol.116.103416
This article has not been copyedited and formatted. The final version may differ from this version.

Introduction

Prostate cancer (PCa) is the second leading cause of cancer-related deaths in men in the United States (Siegel et al., 2015). PCa is initially managed with surgery, radiation, androgen antagonists (e.g., bicalutamide) and surgical or chemical castration. However, the relapsed or metastatic disease post-castration (castration-recurrent prostate cancer or CRPC) has poor prognosis with most patients dying within 2 years (Karantanos et al., 2015). Innovative treatment approaches are urgently needed to treat CRPC patients.

Androgen receptor (AR) signaling is a major driving force in all stages of PCa (Chen et al., 2009). CRPC cells evolve mechanisms to re-activate AR signaling under androgen deprivation conditions (Mitsiades, 2013); these mechanisms include overexpression and gain-of-function mutations of AR (Joseph et al., 2013; Korpal et al., 2013), overexpression of AR splice variants (AR-Vs) (Li et al., 2013), compensatory cross-talk between AR and other signaling pathways (Liu et al., 2014) and enhanced intra-tumoral androgen biosynthesis (Nakamura et al., 2005). Enzalutamide (Enz) is a newly FDA approved AR antagonist that prolongs survival of CRPC patients (Beer et al., 2014; Scher et al., 2012). Enz competitively binds to AR with 5-8 fold higher affinity than bicalutamide and, in contrast to bicalutamide, does not promote AR nuclear translocation (Tran et al., 2009). Nevertheless, acquired resistance to Enz typically develops within months and is associated with a relatively short-lived patient survival benefit. Indeed, *in vivo* generated CRPC cell line models that vastly overexpress AR (e.g., C4-2 cells), presumably in combination with changes in other cellular signaling pathways, are completely resistant to Enz in conditioned media while remaining addicted to AR (Patki et al., 2016).

A possible strategy to overcome resistance to androgen depletion is to induce destabilization and degradation of AR and its associated proteins in CRPC cells. AR is stabilized in the cytosol by its interaction with heat shock protein 90 (HSP90) and other chaperone proteins. HSP90 is commonly overexpressed in many types of cancer cells and has

Molecular Pharmacology Fast Forward. Published on July 5, 2016 as DOI: 10.1124/mol.116.103416
This article has not been copyedited and formatted. The final version may differ from this version.

been explored as a drug target for cancer treatment, including PCa (Bhat et al., 2014; Neckers and Workman, 2012). HSP90 is an ATP-dependent molecular chaperone that aids the folding and stability of a number of client proteins, such as steroid receptors, protein kinases, transcription factors and proteins involved in regulating cell survival. Therefore, inhibition of HSP90 leads to degradation of its client proteins via the ubiquitin-proteasome pathway. Association of the AR apo-protein with HSP90 is critical for stabilizing AR in a conformation that allows androgen binding (Fang et al., 1996; Veldscholte et al., 1992). In PCa cells, HSP90 inhibitors induce AR degradation and impair AR nuclear translocation while simultaneously reducing the levels of other oncogenic client proteins, such as p-AKT/AKT, EGFR and IGF-IR and survivin (He et al., 2013; Liu et al., 2015; Saporita et al., 2007; Solit et al., 2002). Simultaneous disruption of AR and other aberrant growth/survival networks via HSP90 inhibition is an advantageous treatment strategy for CRPC as this would silence potentially mutually compensatory oncogenic signaling pathways. Despite this attractive scientific rationale, clinical development of HSP90 inhibitors for PCa treatment were disappointing (Heath et al., 2008; Oh et al., 2011; Pacey et al., 2011; Thakur et al., 2015) and was also limited by adverse toxicity to non-target tissues.

One of the actions of histone deacetylase (HDAC) inhibitors (HDACi) is to disrupt HSP90 activity. HDACs remove acetyl groups from lysine residues of histone and non-histone proteins. Eighteen HDACs categorized into four classes have been identified in mammalian cells. Among them, HDAC6 is a zinc-dependent, class-IIb HDAC and is localized in the cytoplasm (Kramer et al., 2014). HDAC6 deacetylates HSP90 (Bali et al., 2005; Kovacs et al., 2005). Inhibition of HDAC6 could result in hyper-acetylation of HSP90, loss of ATP binding and dissociation and degradation of its client proteins, including AR. The HDACi LAQ-824 (Chen et al., 2005), PDX-101 (i.e. Belinostat) (Gravina et al., 2013), suberoylanilide hydroxamic acid (SAHA or vorinostat) (Marrocco et al., 2007; Sato et al., 2012) and natural products sulforaphane (Gibbs et al., 2009)

Molecular Pharmacology Fast Forward. Published on July 5, 2016 as DOI: 10.1124/mol.116.103416
This article has not been copyedited and formatted. The final version may differ from this version.

and genistein (Basak et al., 2008) have all been reported to reduce AR protein levels in PCa cells by disrupting the HDAC6-HSP90 chaperone function.

Clinical use of HDACi is now confined to hematological malignancies. Although nuclear HDACs (*e.g.*, HDAC1 and HDAC3) are indispensable for AR transcriptional activity (Welsbie et al., 2009) and increased HDAC levels have been reported in clinical CRPC samples and positively correlated to Gleason scores (Burdelski et al., 2015; Weichert et al., 2008), they are not likely to serve as effective drug targets to treat PCa. HDACi, such as vorinostat (SAHA) (Bradley et al., 2009), romidepsin (FK-228) (Molife et al., 2010), panobinostat (LBH-589) (Rathkopf et al., 2013) and pracinostat (SB-939) (Eigl et al., 2015) have been tested in CRPC patients but have resulted in modest outcomes. Toxicities associated with their pleiotropic effects could contribute to the ineffectiveness of HDACi in PCa treatment. Moreover, recent studies have associated the pleiotropic effects of HDACi, particularly epigenetic modifications of chromatin-associated proteins, with induction of epithelial to mesenchymal transition (EMT) in prostate, endometrial and nasopharyngeal cancer cells (Jiang et al., 2013; Kong et al., 2012; Tam and Weinberg, 2013; Uchida et al., 2012). Therefore clinical translation of the extensive and promising pre-clinical findings of the efficacies of HDACi in treating solid tumors must address the issue of toxicities that prevent application of effective HDACi treatment regimens in the clinic.

We sought to develop enzalutamide derivatives armed with HDACi activity to antagonize AR and HSP90 actions in AR-overexpressing and enzalutamide resistant CRPC cells with reduced pleiotropic effects typical of strong HDACis. Accordingly, we have designed, synthesized and tested the prototype compounds **2-75** and **1005**. The **2-75** and **1005** chemical scaffolds are designed to retain AR binding affinity. The compounds are also designed to have lower intrinsic HDACi activity compared to SAHA, thus reducing the HDACi activity against non-target proteins. Nevertheless, the HDACi activity is expected to produce effective disruption of

Molecular Pharmacology Fast Forward. Published on July 5, 2016 as DOI: 10.1124/mol.116.103416
This article has not been copyedited and formatted. The final version may differ from this version.

AR as well as other HSP90 client proteins, resulting in loss of viability in Enz-resistant CRPC cells.

Molecular Pharmacology Fast Forward. Published on July 5, 2016 as DOI: 10.1124/mol.116.103416
This article has not been copyedited and formatted. The final version may differ from this version.

Materials and Methods

Compound Synthesis. Detailed procedures for the synthesis of compounds **2-75**, **1005**, **3-52** and **1002** are described under Supplemental Materials. The chemical identities of the compounds were confirmed by using ^{1}H, ^{13}C-NMR and high resolution mass spectrometry.

HDAC activity assay. In *vitro* HDAC inhibition was measured by using the HDAC fluorimetric assay/drug discovery Kit (Enzo Life Sciences, BML-AK500) and the HDAC6 fluorometric drug discovery kit (Enzo Life Sciences, BML-AK516) following the manufacturer's protocols and instructions. IC_{50} values were calculated from nonlinear aggression plots using GraphPad Prism5 software.

Cell Culture and Reagents. LNCaP and PC3 cell lines were from American Type Culture Collection (Manassas, Va). LNCaP and C4-2 cells were routinely grown at 37°C in 5% CO_2 in RPMI 1640 medium supplemented with 10% FBS (Invitrogen); 100units/ml penicillin, 100 µg/ml streptomycin, 2mM L-glutamine mixture (Invitrogen); and sodium pyruvate (1mM) (Invitrogen). PC3 cells were grown in RPMI 1640 medium supplemented with 10% FBS (Invitrogen); 100units/ml penicillin, 100 µg/ml streptomycin, 2mM L-glutamine mixture (Invitrogen). Affinity-purified rabbit anti-human antibody to AR (sc-816), mouse anti-human antibody to GAPDH (sc-47724) and affinity-purified mouse anti-human antibody to alpha tubulin (sc-8035) were purchased from Santa Cruz Biotechnology (Santa Cruz, CA). Affinity-purified rabbit anti-human antibody to HSP90 (C45G5) #4877, rabbit anti-human antibody to acetylated lysine #9441, and affinity-purified rabbit anti-human antibody to p21 Waf1/Cip1 #2947S were purchased from Cell Signaling Technology. Affinity-purified rabbit anti-human antibody to acetyl-tubulin (#ABT241), acetyl Histone H4 (#07-328), acetyl Histone H3 (#ABE18) were purchased from Millipore. R1881 was kindly provided by Dr. Stephan Patrick (Karmanos Cancer Institute). Cycloheximide

Molecular Pharmacology Fast Forward. Published on July 5, 2016 as DOI: 10.1124/mol.116.103416
This article has not been copyedited and formatted. The final version may differ from this version.

was from Sigma. All experiments were conducted using phenol-red free growth media. For hormone depletion, cells were grown in phenol-red free RPMI 1640 medium supplemented with 10% charcoal stripped FBS (Sigma-Aldrich) which was heat inactivated at 56°C for thirty minutes, and a mixture of 100units/ml penicillin, 100 µg/ml streptomycin and 2 mM L-glutamine for 96 h.

Cell Viability Assay. Cells were trypsinized and 6000 cells/well were seeded in 96-well plates coated with poly-D-lysine. The cells were seeded in phenol red-free medium supplemented with 10% FBS, 100units/ml penicillin, 100 µg/ml streptomycin, 2mM L-glutamine mixture and sodium pyruvate (1mM) for C4-2 cells and phenol red-free medium supplemented with 10% FBS, 100units/ml penicillin, 100 µg/ml streptomycin and 2mM L-glutamine mixture for PC3 cells. The cells were grown at 37°C in 5% CO_2. Twenty four hours after seeding in the 96-well plates, the cells were treated with indicated compound or DMSO (vehicle). The culture medium was not changed during the time course of the assay. On Day zero and on Day 3, cell viability was determined using the MTT assay. MTT (10µL, 5mg/mL) was added to each well and incubated for 2h at 37°C. The formazan crystal sediments were dissolved in 100µL of DMSO, and the absorbance at 570nm was measured using the BioTek Synergy 2 Microplate Reader (BioTek, Winooski, VT). The assay was conducted in sextuplicate wells and values were normalized to day zero (Patki et al., 2014). IC_{50} values were calculated from nonlinear aggression plots using GraphPad Prism5 software.

Western Blot Analysis. Cells were washed once with phosphate buffered saline (PBS) and then lysed with RIPA buffer (150mM NaCl, 1% Nonidet P-40, 0.5% sodium deoxycholate, 0.1% SDS, 50mM Tris of pH 8.0) containing a protease inhibitor cocktail (Pierce, Thermo Fisher Scientific). The cell lysates were then incubated on ice for 40 minutes. Total protein concentrations were estimated using the Bradford Assay (Bio-Rad). Protein samples (10-40 ug)

Molecular Pharmacology Fast Forward. Published on July 5, 2016 as DOI: 10.1124/mol.116.103416
This article has not been copyedited and formatted. The final version may differ from this version.

were heated at 95°C for 5 minutes and resolved by electrophoresis on 8% polyacrylamide-SDS gels and electrophoretically transferred to PVDF membranes (Millipore, Billerica, MA). The membranes were then probed overnight at 4°C with the appropriate primary antibody followed by the appropriate horseradish peroxidase-conjugated secondary antibody. The blots were then developed to visualize the protein bands using the HyGLO Chemiluminescent HRP Antibody Detection Reagent (Denville Scientific, Metuchen, NI) (Salazar et al., 2011).

RNA isolation, Reverse Transcription, and Real Time PCR. Total RNA was isolated from cells using the RNeasy Mini Kit (Qiagen). Reverse transcription PCR was then performed using 500 ng of total RNA with random primers and using the high-capacity complementary DNA Archive kit (Applied Biosystems). The complementary DNA from this reaction was measured using quantitative real time PCR using the StepONE Plus Real Time PCR system (Life Technologies Corporation, Carlsbad, CA). All reactions were performed in triplicate and normalized to glyceraldehyde-3-phosphate-dehydrogenase values in the same samples. All primers and Taqman probes were purchased from the applied Biosystems inventory (Invitrogen) (Patki et al., 2015).

Chromatin Immunoprecipitation (ChIP). C4-2 cells were treated with either vehicle, R1881 (1 nM or 10 nM), or 10uM of each indicated compound for 2 h and then subjected to ChIP using anti-AR antibody (sc-816 from Santa Cruz, CA). The ChIP assay was performed using the EX ChIP chromatin immunoprecipitation kit (catalogue number 17-371 from Millipore, Temecula,CA) according to the vendor's protocol. The ChIP signals were measured by quantitative real time PCR analysis of the immunoprecipitated products. Each sample was tested in triplicate (Patki et al., 2013).

Molecular Pharmacology Fast Forward. Published on July 5, 2016 as DOI: 10.1124/mol.116.103416
This article has not been copyedited and formatted. The final version may differ from this version.

Statistical Analysis. All experiments were performed in triplicate groups and repeated at least three times. The error bars in all graphs represent the standard deviation. Statistical analysis was performed using one-way ANOVA with post-hoc and LSD (Least Square Differences) and/or T-test (McFall et al., 2015).

Results

Design and synthesis of compounds 2-75 and 1005 with partial chemical scaffolds of Enz and SAHA. Compounds **2-75** and **1005** were designed to retain partial functional scaffolds of Enz and SAHA (Figure 1A). Upon binding to AR, the cyano group of Enz/Enz derivatives forms a critical hydrogen bond with Arg752, and the conformationally restricted thiohydantoin ring in the middle forces the rest of the molecule to the "H11 pocket", a region near the C terminus of helix 11 and the loop connecting helices 11 and 12 (Balbas et al., 2013). To design derivatives with both AR-binding and HDACi activities, different linkers connecting Enz and a zinc binding group (ZBG) were introduced to retain the above structural features that are required for AR binding in an antagonist-related conformation. **1005** is a cinnamyl hydroxamic acid derivative with a three-carbon linker. A relatively longer carbon chain in **2-75** was used to more closely mimic the chemical structure of SAHA. Compound **7** (**3-52**), a close structural analogue of **2-75** using methyl ester to replace ZBG was synthesized as a control compound without an HDACi functional group (Figure 1B). Compound **7** (**3-52**) and synthetic intermediate compound **2** (i.e. **1002,** an ethyl ester analogue of **1005**, Figure 1A, B) were used to investigate AR antagonist properties of **2-75** and **1005** scaffold, respectively.

Both **2-75** and **1005** were synthesized from a 4'-iodo substituted intermediate (Figure 1B) **1**. Acrylate linker of **1005** was introduced via $Pd(OAc)_2$-catalyzed Heck reaction to afford compound **2**, followed by hydrolysis of ethyl ester, coupling to THP (tetrahydropyranyl acetal)-protected hydroxylamine and the final acidic deprotection. To synthesize **2-75**, carboxylation of aryl iodine **1** was performed using a palladium-catalyzed carboxylation reaction (Cacchi et al.,

Molecular Pharmacology Fast Forward. Published on July 5, 2016 as DOI: 10.1124/mol.116.103416
This article has not been copyedited and formatted. The final version may differ from this version.

2003), the resulted carboxylic acid then coupled with primary amines to attach the alkyl chain with protected hydroxamic acid (compound **6**) or methyl ester (compound **7**). Removal of THP protecting group gave the final product **2-75**. The detailed synthetic procedures are described in the Supplemental Material.

Compounds 2-75 and 1005 possess intrinsically weak inhibitor activity against nuclear HDACs and cytosolic HDAC6. To measure HDAC inhibitory activities of **2-75** and **1005**, cell-free enzymatic assays were performed against a nuclear extract of Hela cells and also against human recombinant HDAC6. HDAC1 and HDAC2 are enriched in nuclear extracts whereas HDAC6 is a cytosolic enzyme that is the principal modulator of the acetylation status of HSP90. The HeLa cell nuclear extract was used to evaluate inhibitory activity against nuclear HDACs. **2-75** and **1005** dose-dependently inhibited HDACs enriched in the Hela nuclear extract with IC_{50} values of 1.08 μM and 2.41 μM compared to a value of 0.30 μM for SAHA (Figure 2A). In contrast, compounds **3-52** and **1002**, which share the chemical scaffolds of **2-75** and **1005** respectively, but lack the HDACi functional group, did not inhibit nuclear HDAC activity even up to a concentration of 25 μM (Figure 2B). As expected, Enz also lacked any HDACi activity in contrast to a pan-HDACi, trichostatin A (TSA), which was used as a positive control (Figure 2B). **2-75** and **1005** were also weaker inhibitors of recombinant HDAC6, with IC_{50} values of 2.0 μM and 6.93 μM, respectively compared with the IC_{50} of 0.85 μM for SAHA (Figure 2C). As expected, the negative control compounds **3-52** and **1002** as well as Enz did not show significant inhibitory activity against HDAC6 even at a concentration of 25 μM (Figure 2D). Again, TSA served as the positive control in Figure 2D.

The HDACi activities of **2-75** and **1005** were also compared with those of their parent compounds *in situ* in both LNCaP and C4-2 prostate cancer cells using activation of the DLC1 tumor suppressor gene as the readout. SAHA induces histone acetylation at the DLC1 promoter and effectively increases DLC1 mRNA expression in prostate cancer cells (Zhou et al., 2012).

Molecular Pharmacology Fast Forward. Published on July 5, 2016 as DOI: 10.1124/mol.116.103416
This article has not been copyedited and formatted. The final version may differ from this version.

Accordingly, DLC1 mRNA was strongly up-regulated by SAHA in both LNCaP cells (Figure 2E) and in C4-2 cells (Figure 2F). As expected from the fact that DLC1 is not an AR-regulated gene, Enz had no effect on DLC1 mRNA expression. Consistent with the results of the cell-free HDACi assays above, compounds **2-75** and **1005** were poor inducers of DLC1 mRNA compared with SAHA, both in LNCaP cells and in C4-2 cells (Figure 2E and 2F). Further, similar to the results from cell-free assays, **1005** was a much weaker HDACi than **2-75** in the *in situ* assays (Figure 2E and 2F). Taken together, the results indicate that compounds **2-75** and, to a greater degree, **1005** have much less potent HDACi activity in the cellular context reflecting their intrinsically weak inhibitor activities compared with SAHA.

The partial Enz chemical scaffold confers AR targeted antagonist activity without ligand-induced chromatin association of AR. Although C4-2 cells are not growth-inhibited by Enz due to hormone-independent actions of AR, the canonical androgen target genes KLK3 and TMPRSS2 are activated by androgen and their activation is inhibited by androgen antagonists (Ratnam et al., 2013). HDACi are also potent inhibitors of the androgen signaling axis as they cause degradation of AR in the cytosol in addition to other cellular effects (Chen et al., 2005; Gravina et al., 2013; Gryder et al., 2013). To test whether the Enz moiety could enable **2-75** and **1005** to target to AR, we tested the ability of compound **3-52** to inhibit activation of KLK3 and TMPRSS2 by androgen. Compound **3-52** shares the chemical scaffold of **2-75** but lacks the HDACi functional group; therefore **3-52** should depend on the partial Enz chemical scaffold to antagonize gene activation by androgen. SAHA partially inhibited activation of KLK3 (Figure 3A) and TMPRSS2 (Figure 3B) by the synthetic androgen R1881 in C4-2 cells whereas Enz showed progressive inhibition at higher doses. Compounds **2-75** and **1005** were both better inhibitors of gene activation by androgen compared with either Enz or SAHA (Figure 3A and 3B). On the other hand, compound **3-52** inhibited activation of KLK3 and TMPRSS2 to a degree that was comparable to Enz suggesting that the partial Enz chemical scaffold in compounds **2-75** and

Molecular Pharmacology Fast Forward. Published on July 5, 2016 as DOI: 10.1124/mol.116.103416
This article has not been copyedited and formatted. The final version may differ from this version.

1005 retained an Enz-like AR binding property. The superior androgen antagonist activities of **2-75** and **1005** compared with Enz may be explained by their additional HDACi activities.

AR ligands including agonists and classical androgen antagonists such as bicalutamide promote nuclear translocation of AR and the binding of AR to canonical hormone (androgen) response elements associated with androgen-regulated genes. In contrast, Enz does not stimulate AR nuclear translocation and DNA binding (Guerrero et al., 2013; Tran et al., 2009). To test whether the partial Enz chemical scaffold would mobilize AR to the chromatin, we employed chromatin immunoprecipitation using C4-2 cells treated with androgen, Enz, SAHA and compound **2-75**. As a target site for the ChIP assay, we chose the well-established AR binding enhancer elements located 4kb upstream of the transcription initiation site of the KLK3 gene. As seen in Figure 3C, androgen treatment strongly stimulated chromatin association of AR whereas Enz, SAHA and compound **2-75** all gave the basal ChIP signal corresponding to the vehicle treatment control. These results suggest that the new compounds must antagonize AR in the cytosolic rather than in the nuclear compartment.

Compounds 2-75 and 1005 induce enhanced degradation of AR and HSP90 and hyper-acetylation in a putative 55 KDa HSP90 fragment. Previous observations using potent non-targeted HDACi have shown that the compounds directly affect the AR signaling axis by hyper-acetylation of the AR chaperone complex, through inhibition of HDAC6, leading to degradation of HSP90 as well as release and degradation of AR. We therefore hypothesized that despite their intrinsically weak HDACi activities, the Enz moiety may enable compounds **2-75** and **1005** to more effectively target AR in its chaperone complex, leading to relatively efficient degradation of AR. To test this possibility, we treated C4-2 cells with Enz, SAHA, **1005** and **2-75** at doses ranging from 1μM to 10μM for 24h. Western blots of the cell lysates were probed for AR and GAPDH (loading control) and the AR band intensities relative to GAPDH were quantified using ImageJ software (Figure 4A). Whereas Enz did not cause an appreciable change in the AR

Molecular Pharmacology Fast Forward. Published on July 5, 2016 as DOI: 10.1124/mol.116.103416
This article has not been copyedited and formatted. The final version may differ from this version.

protein level, SAHA did cause a decrease in AR level in a dose-dependent manner (Figure 4A). Compared to SAHA, both **2-75** and **1005** decreased the AR level to a greater extent with **2-75** being more effective than **1005** at each dose (Figure 4A). To determine whether the decrease in AR was due to increase in the rate of AR degradation we tested the effects of the compounds after blocking *de novo* protein synthesis using cycloheximide. We monitored degradation of p21 to confirm the activity of cycloheximide. As expected there was a rapid decrease in p21 upon treatment with cycloheximide confirming that the treatment efficiently blocked *de novo* protein synthesis (Figure 5). In the presence of cycloheximide the AR protein level was decreased by approximately half at the end of 24h indicating a relatively slow turnover of the AR protein. Under these conditions treatment with SAHA, 1005 and 2-75 all caused greater declines in the AR level with 2-75 showing the strongest effect (Figure 5). The results indicate that the decrease in AR caused by 1005 and 2-75 is due to increased degradation of AR. The extent of degradation of AR in C4-2 cells appeared adequate to offset the high level of overexpression of AR that is necessary to support growth in these cells.

To explore a possible link between decreased AR levels and effects of the compounds on the AR chaperone complex, we examined whether compounds **2-75** and **1005** decreased the level of HSP90. Probing of the lysates from the treated cells (48h treatment) for HSP90 by western blot and quantification of HSP90 was conducted by procedures similar to that used above for AR. Enz had no effect on the level of HSP90 whereas in the SAHA-treated cells, a decrease in HSP90 was evident at the higher doses (5μM and 10μM) (Figure 4B). On the other hand, cells treated with **1005** and **2-75** showed more marked reduction in HSP90, with **2-75** being more efficient than **1005**. Probing identical western blots with an antibody against acetylated lysine showed that SAHA as well as **1005** and **2-75,** but not Enz, showed hyper-acetylation of a ~55 KDa polypeptide (Figure 4C), similar to one that has previously been identified as a fragment HSP90 produced by SAHA treatment (Park et al., 2015). Taken together, the above results are consistent with the view that the ability of the compounds to

Molecular Pharmacology Fast Forward. Published on July 5, 2016 as DOI: 10.1124/mol.116.103416
This article has not been copyedited and formatted. The final version may differ from this version.

induce acetylation and reduction of HSP90, and consequently AR degradation, underlies the ability of the compounds to attenuate AR signaling.

The hybrid molecules selectively inhibit cytosolic HDAC6 *in situ*. As HSP90 in the AR chaperone complex is a target of the cytosolic HDAC6, the hyper-acetylation of degradation of HSP90 induced by **2-75** and **1005** is likely to occur through inhibition of HDAC6. If this were the case, we may expect that **2-75** and **1005** would also induce hyper-acetylation of α-tubulin which is diagnostic of HDAC6 inhibition. To test this possibility, we treated C4-2 cells with Enz, SAHA, **1005** and **2-75** at doses ranging from 2.5μM to 10μM for 24h. Western blots of the cell lysates were probed for acetyl-tubulin, as well as total α-tubulin. The band intensities for acetyl-tubulin relative to total α-tubulin were quantified using ImageJ software (Figure 6). **2-75** induced a greater degree of hyper-acetylation of α-tubulin (relative to total tubulin) compared to SAHA, whereas 1005 produced a similar effect albeit to a somewhat lesser degree than SAHA (Figure 6). When the same cell lysates were probed using antibodies against acetylated histones H3 and H4, it was clear that SAHA alone induced a strong induction of histone acetylation (Figure 6). The results clearly demonstrate strong and selective *in situ* activity of **2-75** and **1005** on cytosolic HDAC6.

2-75 and 1005 up-regulate p21 and inhibit viability of Enz-resistant prostate cancer cells. HDACi activate transcription of p21. However, as compounds **2-75** and **1005** exhibited weak intrinsic HDACi activity against nuclear HDACs and as their apparent major cellular HDACi activity was related to targeting of the AR axis within the cytosolic compartment, it was of interest to examine their ability to induce p21.

Enz had no effect on p21 mRNA expression in either the Enz-sensitive LNCaP cells (Figure 7A) or in the Enz-insensitive C4-2 cells (Figure 7B), whereas SAHA induced p21 mRNA in both cell lines (Figure 7A and 7B). Compounds **2-75** and **1005** both induced p21 to a greater extent than SAHA in the two cell lines (Figure 7A and 7B). Moreover, combined treatment with

Molecular Pharmacology Fast Forward. Published on July 5, 2016 as DOI: 10.1124/mol.116.103416
This article has not been copyedited and formatted. The final version may differ from this version.

equimolar concentrations of Enz and SAHA did not induce p21 to a greater extent than SAHA alone, indicating the importance of the hybrid scaffold of **2-75** and **1005** (Figure 7C).

To expect therapeutic effects from **2-75** and **1005**, it is important to establish that, similar to SAHA, they can induce loss of viability in Enz-resistant CRPC cells, rather than mere growth inhibition. Therefore, the effects of **2-75**, **1005** and SAHA on cell viability were assessed in the well-established C4-2 model of Enz-resistant CRPC.

In C4-2 cells Enz could not appreciably affect viability even at a concentration of 10 μM, whereas SAHA caused loss of viability in a dose dependent manner (Figure 8A). Compounds **2-75** and **1005** both caused greater loss of viability compared with SAHA with compound **2-75** being more effective than **1005** (Figure 8A). As a control, compound **1002**, which has a chemical scaffold similar to **1005** but lacks the HDACi activity (Figure 2B and 2D), was unable to affect C4-2 cell viability (Figure 8A). As another experimental control, at the lower drug concentration (2.5 uM) although SAHA, **2-75** and **1005** caused growth inhibition, combining Enz with SAHA (each at 2.5 uM) did not enhance the ability of SAHA to inhibit cell growth (Figure 8B). In the AR-negative PC3 PCa cells, SAHA induced loss of viability in a dose-dependent manner (Figure 8C). However, in contrast to C4-2 cells, neither **2-75** nor **1005** affected viability of PC3 cells within the duration of the assay (Figure 8C). As expected, the AR-positive and hormone-dependent LNCaP cells were sensitive to SAHA, **2-75** and **1005** as well as Enz (Supplemental Figure 1).

The results indicate that despite the weaker inherent HDACi activities of **2-75** and **1005** compared with SAHA, the compounds could be as good or better at reducing viability of Enz-resistant and AR-overexpressing PCa cells.

Molecular Pharmacology Fast Forward. Published on July 5, 2016 as DOI: 10.1124/mol.116.103416
This article has not been copyedited and formatted. The final version may differ from this version.

Discussion

The success of clinical interventions in prostate cancer, including surgical or chemical castration and treatment with androgen antagonists and androgen synthesis inhibitors support the view that the majority of prostate tumors are addicted to AR to support PCa growth and progression (Zegarra-Moro et al., 2002). Nevertheless, the current interventions that target androgen/AR signaling are circumvented by the tumors, most commonly through mechanisms that restore functional AR (Feldman and Feldman, 2001; Yuan and Balk, 2009), resulting in short-lived clinical benefit from the treatments. The goal of this study was to develop a class of compounds that may overcome this manner of resistance to the conventional treatments by efficiently disrupting both AR and HSP90 in the AR-HSP90 complex with minimal effects on most other cellular targets. To accomplish this, we synthesized compounds that would incorporate properties of two well-known drugs, an HDACi (SAHA) that efficiently modifies and disrupts the cytosolic AR chaperone complex and an AR ligand (Enz), which is a high affinity AR antagonist. We additionally sought to substantially weaken the intrinsic HDACi activity of the drug to minimize its ability to affect many targets. The studies described above suggest that compounds **2-75** and **1005** may be prototype molecules that fit this paradigm.

The HDACi functional groups in **2-75** and **1005** conferred only weak HDACi activity in cell-free assays using either nuclear HDACs or the cytosolic HDAC6 compared with SAHA; the shorter carbon chain in **1005** resulted in even weaker HDACi activity than **2-75**. The relative potencies of HDACi inhibition of **2-75** and **1005** was clearly reflected in their relatively poor ability to induce DLC1, an established nuclear target gene of HDACi (Guan et al., 2006; Zhou et al., 2010; Zhou et al., 2012), that is strongly induced by SAHA. **2-75** and **1005** were also poor modulators of histone acetylation *in situ* compared with SAHA. Therefore, the new molecules may have less toxic effects than those associated with the potent pan-HDACi activity of SAHA (Bradley et al., 2009).

Molecular Pharmacology Fast Forward. Published on July 5, 2016 as DOI: 10.1124/mol.116.103416
This article has not been copyedited and formatted. The final version may differ from this version.

SAHA partially inhibited gene activation by androgen but did not produce a further dose-dependent inhibition between 1μM and 10 μM concentrations. At this time, we do not have a clear explanation for why this effect of SAHA was only partial except that it may be related to the pleiotropic cellular effects of SAHA including its effects on cross-talking molecular pathways. More important, **2-75** and **1005** produced a dose-dependent inhibition of gene activation by androgen similar to Enz. The stronger inhibition observed for the compounds compared to Enz may be attributed to their HDACi moieties. However, the close parallel between the control compound **3-52** and Enz in their dose-dependent antagonism of gene activation by androgen, despite the lack of a HDACi functional group in **3-52**, indicates that the Enz moiety in **2-75** and **1005** is functional in enabling binding to AR. Additionally, ChIP analysis showed that the modified Enz scaffold retained the inability of Enz to mobilize AR to its chromatin binding sites in the nucleus in contrast to conventional androgen antagonists.

In the context of targeted delivery to AR via their Enz moiety, the weak intrinsic HDACi activities of **2-75** and **1005** were adequate to mimic or surpass the effects of SAHA on AR protein levels. The efficiency of degradation of AR by **1005** was comparable to SAHA but **2-75** clearly induced AR degradation to a greater degree at each dose. This difference between **2-75** and **1005** may be related to the fact that the HDACi activity of **1005** was less than that of **2-75**, despite their common Enz moiety. To test the mechanism by which **2-75** and **1005** may cause AR degradation, we relied on literature reports that HDACi destabilize and degrade AR by hyper-acetylating and inducing degradation of the cytosolic AR chaperone protein, HSP90 (Chen et al., 2005; Gravina et al., 2013; Gryder et al., 2013). It has also been reported that the hyper-acetylation and degradation of HSP90 coincides with the appearance of a ~55 KDa HSP90 polypeptide fragment. As a diagnostic test of this mechanism, we observed that similar to SAHA, **2-75** and **1005** did indeed cause a decrease in HSP90, with **2-75** being more efficient than either SAHA or **1005**. We were able to observe the predicted ~55KDa fragment in cells treated with SAHA, **2-75** or **1005** using an antibody against acetylated lysine; however our

Molecular Pharmacology Fast Forward. Published on July 5, 2016 as DOI: 10.1124/mol.116.103416
This article has not been copyedited and formatted. The final version may differ from this version.

antibody against HSP90 was unable to detect this fragment, possibly because the levels of the cleaved HSP90 fragment were too low to be in the detectable range of the antibody. Nevertheless, all indications point to the AR chaperone complex in the cytosol as the mediating the action of **2-75** and **1005**. Consistent with this view HDAC6 which is associated with the AR-HSP90 complex was more strongly and selectively inhibited *in situ* by **2-75** compared to SAHA. Indeed **1005** which had weaker intrinsic HDACi activity than **2-75** also strongly inhibited HDAC6 *in situ* with virtually no effect on histone acetylation.

An increase in the expression of the cyclin-dependent kinase inhibitor p21 (Gartel and Tyner, 2002) is a hall mark of the antiproliferative effects of HDACi (Gui et al., 2004; Marks, 2004). Potent inhibition of the nuclear HDAC1 at the promoter of the p21 gene is associated with induction of p21 by HDACi (Lagger et al., 2003). Inhibitors of HSP90 also increase p21 expression in PCa cells (Chen et al., 2005). Therefore it is significant that p21 mRNA was induced by both **2-75** and **1005** more strongly than SAHA and that combination with Enz did not further increase p21 induction by SAHA. The inability of Enz to induce p21 in the hormone-dependent LNCaP cells despite the sensitivity of the AR signaling in these cells to Enz suggests that induction of p21 by **2-75** and **1005** may not be directly related to disruption of AR; rather, it may be due to their effects on additional HSP90 client proteins through AR-mediated targeting of HDACi activity to HSP90. Notably, AKT and GR are also HSP90 client proteins and upregulated AKT or GR signaling were reported to result in Enz resistance (Arora et al., 2013; Bitting and Armstrong, 2013; Montgomery et al., 2015; Toren et al., 2015),. Therefore, these pathways could be involved in the loss of viability induced by the compounds.

HDACi pharmacophores have previously been linked to a chemical scaffold of cyanonilutamide, which is another nonsteroidal AR antagonist (Gryder et al., 2013). However, the antiproliferative effects of cyanonilutamide-HDACi were related to their ability to induce AR nuclear localization, enabling elevated local concentrations of HDACi activities in the nucleus. In

Molecular Pharmacology Fast Forward. Published on July 5, 2016 as DOI: 10.1124/mol.116.103416
This article has not been copyedited and formatted. The final version may differ from this version.

contrast, our prototype drug molecules were designed to limit nuclear HDACi activities as an approach to limiting toxicity. Our working model that would need further testing is that in C4-2 cells, **2-75** and **1005** bind to cytosolic AR and inhibit HDAC6 associated with the AR chaperone complex, resulting in HSP90 acetylation and degradation, AR degradation, suppression of ligand-insensitive gene activation by AR and inhibition HSP90 interactions with additional client proteins (Schematic in Figure 9). We propose that this mechanism may address some of the limitations of strong pan-HDAC inhibitors related to toxicity.

Molecular Pharmacology Fast Forward. Published on July 5, 2016 as DOI: 10.1124/mol.116.103416
This article has not been copyedited and formatted. The final version may differ from this version.

Acknowledgements

We thank Yanfang Huang for technical support.

Authors' Contributions

Participated in research design: Rosati, Chen, Patki, Ou, McFall, Ratnam, Qin

Conducted experiments: Rosati, Chen, Patki, Ou, Qin

Contributed new reagents or analytic tools: Rosati, Chen, Ou, Heath, McFall, Ratnam, Qin

Performed data analysis: Rosati, Chen, Ou, McFall, Ratnam, Qin

Wrote or contributed to the writing of the manuscript: Rosati, Chen, Ratnam, Qin

Molecular Pharmacology Fast Forward. Published on July 5, 2016 as DOI: 10.1124/mol.116.103416
This article has not been copyedited and formatted. The final version may differ from this version.

References

Arora, V. K., Schenkein, E., Murali, R., Subudhi, S. K., Wongvipat, J., Balbas, M. D., Shah, N., Cai, L., Efstathiou, E., and Logothetis, C. (2013). Glucocorticoid receptor confers resistance to antiandrogens by bypassing androgen receptor blockade. Cell *155*, 1309-1322.

Balbas, M. D., Evans, M. J., Hosfield, D. J., Wongvipat, J., Arora, V. K., Watson, P. A., Chen, Y., Greene, G. L., Shen, Y., and Sawyers, C. L. (2013). Overcoming mutation-based resistance to antiandrogens with rational drug design. eLife *2*, e00499.

Bali, P., Pranpat, M., Bradner, J., Balasis, M., Fiskus, W., Guo, F., Rocha, K., Kumaraswamy, S., Boyapalle, S., Atadja, P.*, et al.* (2005). Inhibition of histone deacetylase 6 acetylates and disrupts the chaperone function of heat shock protein 90: a novel basis for antileukemia activity of histone deacetylase inhibitors. The Journal of biological chemistry *280*, 26729-26734.

Basak, S., Pookot, D., Noonan, E. J., and Dahiya, R. (2008). Genistein down-regulates androgen receptor by modulating HDAC6-Hsp90 chaperone function. Molecular cancer therapeutics *7*, 3195-3202.

Beer, T. M., Armstrong, A. J., Rathkopf, D. E., Loriot, Y., Sternberg, C. N., Higano, C. S., Iversen, P., Bhattacharya, S., Carles, J., Chowdhury, S.*, et al.* (2014). Enzalutamide in metastatic prostate cancer before chemotherapy. The New England journal of medicine *371*, 424-433.

Bhat, R., Tummalapalli, S. R., and Rotella, D. P. (2014). Progress in the discovery and development of heat shock protein 90 (Hsp90) inhibitors. Journal of medicinal chemistry *57*, 8718-8728.

Bitting, R. L., and Armstrong, A. J. (2013). Targeting the PI3K/Akt/mTOR pathway in castration-resistant prostate cancer. Endocrine-related cancer *20*, R83-R99.

Bradley, D., Rathkopf, D., Dunn, R., Stadler, W. M., Liu, G., Smith, D. C., Pili, R., Zwiebel, J., Scher, H., and Hussain, M. (2009). Vorinostat in advanced prostate cancer patients progressing on prior chemotherapy (National Cancer Institute Trial 6862): trial results and interleukin-6

analysis: a study by the Department of Defense Prostate Cancer Clinical Trial Consortium and University of Chicago Phase 2 Consortium. Cancer *115*, 5541-5549.

Burdelski, C., Ruge, O. M., Melling, N., Koop, C., Simon, R., Steurer, S., Sauter, G., Kluth, M., Hube-Magg, C., Minner, S*., et al.* (2015). HDAC1 overexpression independently predicts biochemical recurrence and is associated with rapid tumor cell proliferation and genomic instability in prostate cancer. Experimental and molecular pathology *98*, 419-426.

Cacchi, S., Fabrizi, G., and Goggiamani, A. (2003). Palladium-catalyzed hydroxycarbonylation of aryl and vinyl halides or triflates by acetic anhydride and formate anions. Organic letters *5*, 4269-4272.

Chen, L., Meng, S., Wang, H., Bali, P., Bai, W., Li, B., Atadja, P., Bhalla, K. N., and Wu, J. (2005). Chemical ablation of androgen receptor in prostate cancer cells by the histone deacetylase inhibitor LAQ824. Molecular cancer therapeutics *4*, 1311-1319.

Chen, Y., Clegg, N. J., and Scher, H. I. (2009). Anti-androgens and androgen-depleting therapies in prostate cancer: new agents for an established target. The lancet oncology *10*, 981-991.

Eigl, B. J., North, S., Winquist, E., Finch, D., Wood, L., Sridhar, S. S., Powers, J., Good, J., Sharma, M., Squire, J. A*., et al.* (2015). A phase II study of the HDAC inhibitor SB939 in patients with castration resistant prostate cancer: NCIC clinical trials group study IND195. Investigational new drugs *33*, 969-976.

Fang, Y., Fliss, A. E., Robins, D. M., and Caplan, A. J. (1996). Hsp90 regulates androgen receptor hormone binding affinity in vivo. The Journal of biological chemistry *271*, 28697-28702.

Feldman, B. J., and Feldman, D. (2001). The development of androgen-independent prostate cancer. Nature Reviews Cancer *1*, 34-45.

Gartel, A. L., and Tyner, A. L. (2002). The role of the cyclin-dependent kinase inhibitor p21 in apoptosis. Molecular cancer therapeutics *1*, 639-649.

Gibbs, A., Schwartzman, J., Deng, V., and Alumkal, J. (2009). Sulforaphane destabilizes the androgen receptor in prostate cancer cells by inactivating histone deacetylase 6. Proceedings of the National Academy of Sciences of the United States of America *106*, 16663-16668.

Gravina, G. L., Marampon, F., Muzi, P., Mancini, A., Piccolella, M., Negri-Cesi, P., Motta, M., Lenzi, A., Di Cesare, E., Tombolini, V.*, et al.* (2013). PXD101 potentiates hormonal therapy and prevents the onset of castration-resistant phenotype modulating androgen receptor, HSP90, and CRM1 in preclinical models of prostate cancer. Endocrine-related cancer *20*, 321-337.

Gryder, B. E., Akbashev, M. J., Rood, M. K., Raftery, E. D., Meyers, W. M., Dillard, P., Khan, S., and Oyelere, A. K. (2013). Selectively targeting prostate cancer with antiandrogen equipped histone deacetylase inhibitors. ACS chemical biology *8*, 2550-2560.

Guan, M., Zhou, X., Soulitzis, N., Spandidos, D. A., and Popescu, N. C. (2006). Aberrant methylation and deacetylation of deleted in liver cancer-1 gene in prostate cancer: potential clinical applications. Clinical cancer research : an official journal of the American Association for Cancer Research *12*, 1412-1419.

Guerrero, J., Alfaro, I. E., Gomez, F., Protter, A. A., and Bernales, S. (2013). Enzalutamide, an androgen receptor signaling inhibitor, induces tumor regression in a mouse model of castration-resistant prostate cancer. The Prostate *73*, 1291-1305.

Gui, C. Y., Ngo, L., Xu, W. S., Richon, V. M., and Marks, P. A. (2004). Histone deacetylase (HDAC) inhibitor activation of p21WAF1 involves changes in promoter-associated proteins, including HDAC1. Proceedings of the National Academy of Sciences of the United States of America *101*, 1241-1246.

He, S., Zhang, C., Shafi, A. A., Sequeira, M., Acquaviva, J., Friedland, J. C., Sang, J., Smith, D. L., Weigel, N. L., Wada, Y., and Proia, D. A. (2013). Potent activity of the Hsp90 inhibitor ganetespib in prostate cancer cells irrespective of androgen receptor status or variant receptor expression. International journal of oncology *42*, 35-43.

Heath, E. I., Hillman, D. W., Vaishampayan, U., Sheng, S., Sarkar, F., Harper, F., Gaskins, M., Pitot, H. C., Tan, W., Ivy, S. P.*, et al.* (2008). A phase II trial of 17-allylamino-17-demethoxygeldanamycin in patients with hormone-refractory metastatic prostate cancer. Clinical cancer research : an official journal of the American Association for Cancer Research *14*, 7940-7946.

Jiang, G. M., Wang, H. S., Zhang, F., Zhang, K. S., Liu, Z. C., Fang, R., Wang, H., Cai, S. H., and Du, J. (2013). Histone deacetylase inhibitor induction of epithelial-mesenchymal transitions via up-regulation of Snail facilitates cancer progression. Biochimica et biophysica acta *1833*, 663-671.

Joseph, J. D., Lu, N., Qian, J., Sensintaffar, J., Shao, G., Brigham, D., Moon, M., Maneval, E. C., Chen, I., Darimont, B., and Hager, J. H. (2013). A clinically relevant androgen receptor mutation confers resistance to second-generation antiandrogens enzalutamide and ARN-509. Cancer discovery *3*, 1020-1029.

Karantanos, T., Evans, C. P., Tombal, B., Thompson, T. C., Montironi, R., and Isaacs, W. B. (2015). Understanding the mechanisms of androgen deprivation resistance in prostate cancer at the molecular level. European urology *67*, 470-479.

Kong, D., Ahmad, A., Bao, B., Li, Y., Banerjee, S., and Sarkar, F. H. (2012). Histone deacetylase inhibitors induce epithelial-to-mesenchymal transition in prostate cancer cells. PloS one *7*, e45045.

Korpal, M., Korn, J. M., Gao, X., Rakiec, D. P., Ruddy, D. A., Doshi, S., Yuan, J., Kovats, S. G., Kim, S., Cooke, V. G.*, et al.* (2013). An F876L mutation in androgen receptor confers genetic and phenotypic resistance to MDV3100 (enzalutamide). Cancer discovery *3*, 1030-1043.

Kovacs, J. J., Murphy, P. J., Gaillard, S., Zhao, X., Wu, J. T., Nicchitta, C. V., Yoshida, M., Toft, D. O., Pratt, W. B., and Yao, T. P. (2005). HDAC6 regulates Hsp90 acetylation and chaperone-dependent activation of glucocorticoid receptor. Molecular cell *18*, 601-607.

Kramer, O. H., Mahboobi, S., and Sellmer, A. (2014). Drugging the HDAC6-HSP90 interplay in malignant cells. Trends in pharmacological sciences *35*, 501-509.

Lagger, G., Doetzlhofer, A., Schuettengruber, B., Haidweger, E., Simboeck, E., Tischler, J., Chiocca, S., Suske, G., Rotheneder, H., Wintersberger, E., and Seiser, C. (2003). The tumor suppressor p53 and histone deacetylase 1 are antagonistic regulators of the cyclin-dependent kinase inhibitor p21/WAF1/CIP1 gene. Molecular and cellular biology *23*, 2669-2679.

Li, Y., Chan, S. C., Brand, L. J., Hwang, T. H., Silverstein, K. A., and Dehm, S. M. (2013). Androgen receptor splice variants mediate enzalutamide resistance in castration-resistant prostate cancer cell lines. Cancer research *73*, 483-489.

Liu, C., Zhang, Z., Tang, H., Jiang, Z., You, L., and Liao, Y. (2014). Crosstalk between IGF-1R and other tumor promoting pathways. Current pharmaceutical design *20*, 2912-2921.

Liu, W., Vielhauer, G. A., Holzbeierlein, J. M., Zhao, H., Ghosh, S., Brown, D., Lee, E., and Blagg, B. S. (2015). KU675, a Concomitant Heat-Shock Protein Inhibitor of Hsp90 and Hsc70 that Manifests Isoform Selectivity for Hsp90alpha in Prostate Cancer Cells. Molecular pharmacology *88*, 121-130.

Marks, P. A. (2004). The mechanism of the anti-tumor activity of the histone deacetylase inhibitor, suberoylanilide hydroxamic acid (SAHA). Cell cycle *3*, 534-535.

Marrocco, D. L., Tilley, W. D., Bianco-Miotto, T., Evdokiou, A., Scher, H. I., Rifkind, R. A., Marks, P. A., Richon, V. M., and Butler, L. M. (2007). Suberoylanilide hydroxamic acid (vorinostat) represses androgen receptor expression and acts synergistically with an androgen receptor antagonist to inhibit prostate cancer cell proliferation. Molecular cancer therapeutics *6*, 51-60.

McFall, T., Patki, M., Rosati, R., and Ratnam, M. (2015). Role of the short isoform of the progesterone receptor in breast cancer cell invasiveness at estrogen and progesterone levels in the pre- and post-menopausal ranges. Oncotarget *6*, 33146-33164.

Mitsiades, N. (2013). A road map to comprehensive androgen receptor axis targeting for castration-resistant prostate cancer. Cancer research *73*, 4599-4605.

Molife, L. R., Attard, G., Fong, P. C., Karavasilis, V., Reid, A. H., Patterson, S., Riggs, C. E., Jr., Higano, C., Stadler, W. M., McCulloch, W*., et al.* (2010). Phase II, two-stage, single-arm trial of the histone deacetylase inhibitor (HDACi) romidepsin in metastatic castration-resistant prostate cancer (CRPC). Annals of oncology : official journal of the European Society for Medical Oncology / ESMO *21*, 109-113.

Montgomery, B., Kheoh, T., Molina, A., Li, J., Bellmunt, J., Tran, N., Loriot, Y., Efstathiou, E., Ryan, C. J., and Scher, H. I. (2015). Impact of baseline corticosteroids on survival and steroid androgens in metastatic castration-resistant prostate cancer: exploratory analysis from COU-AA-301. European urology *67*, 866-873.

Nakamura, Y., Suzuki, T., Nakabayashi, M., Endoh, M., Sakamoto, K., Mikami, Y., Moriya, T., Ito, A., Takahashi, S., Yamada, S*., et al.* (2005). In situ androgen producing enzymes in human prostate cancer. Endocrine-related cancer *12*, 101-107.

Neckers, L., and Workman, P. (2012). Hsp90 molecular chaperone inhibitors: are we there yet? Clinical cancer research : an official journal of the American Association for Cancer Research *18*, 64-76.

Oh, W. K., Galsky, M. D., Stadler, W. M., Srinivas, S., Chu, F., Bubley, G., Goddard, J., Dunbar, J., and Ross, R. W. (2011). Multicenter phase II trial of the heat shock protein 90 inhibitor, retaspimycin hydrochloride (IPI-504), in patients with castration-resistant prostate cancer. Urology *78*, 626-630.

Pacey, S., Wilson, R. H., Walton, M., Eatock, M. M., Hardcastle, A., Zetterlund, A., Arkenau, H. T., Moreno-Farre, J., Banerji, U., Roels, B*., et al.* (2011). A phase I study of the heat shock protein 90 inhibitor alvespimycin (17-DMAG) given intravenously to patients with advanced solid tumors. Clinical cancer research : an official journal of the American Association for Cancer Research *17*, 1561-1570.

Park, S., Park, J. A., Kim, Y. E., Song, S., Kwon, H. J., and Lee, Y. (2015). Suberoylanilide hydroxamic acid induces ROS-mediated cleavage of HSP90 in leukemia cells. Cell stress & chaperones *20*, 149-157.

Patki, M., Chari, V., Sivakumaran, S., Gonit, M., Trumbly, R., and Ratnam, M. (2013). The ETS domain transcription factor ELK1 directs a critical component of growth signaling by the androgen receptor in prostate cancer cells. The Journal of biological chemistry *288*, 11047-11065.

Patki, M., Gadgeel, S., Huang, Y., McFall, T., Shields, A. F., Matherly, L. H., Bepler, G., and Ratnam, M. (2014). Glucocorticoid receptor status is a principal determinant of variability in the sensitivity of non-small-cell lung cancer cells to pemetrexed. Journal of thoracic oncology : official publication of the International Association for the Study of Lung Cancer *9*, 519-526.

Patki, M., Huang, Y., and Ratnam, M. (2016). Restoration of the cellular secretory milieu overrides androgen dependence of in vivo generated castration resistant prostate cancer cells overexpressing the androgen receptor. Biochemical and biophysical research communications *476*, 69-74.

Patki, M., Salazar, M., Trumbly, R., and Ratnam, M. (2015). Differential effects of estrogen-dependent transactivation vs. transrepression by the estrogen receptor on invasiveness of HER2 overexpressing breast cancer cells. Biochemical and biophysical research communications *457*, 404-411.

Rathkopf, D. E., Picus, J., Hussain, A., Ellard, S., Chi, K. N., Nydam, T., Allen-Freda, E., Mishra, K. K., Porro, M. G., Scher, H. I., and Wilding, G. (2013). A phase 2 study of intravenous panobinostat in patients with castration-resistant prostate cancer. Cancer chemotherapy and pharmacology *72*, 537-544.

Ratnam, M., Patki, M., Gonit, M., and Trumbly, R. (2013). Mechanisms of ARE-Independent Gene Activation by the Androgen Receptor in Prostate Cancer Cells: Potential Targets for

Better Intervention Strategies. In Androgen-Responsive Genes in Prostate Cancer, (Springer), pp. 85-100.

Salazar, M. D., Ratnam, M., Patki, M., Kisovic, I., Trumbly, R., Iman, M., and Ratnam, M. (2011). During hormone depletion or tamoxifen treatment of breast cancer cells the estrogen receptor apoprotein supports cell cycling through the retinoic acid receptor alpha1 apoprotein. Breast cancer research : BCR *13*, R18.

Saporita, A. J., Ai, J., and Wang, Z. (2007). The Hsp90 inhibitor, 17-AAG, prevents the ligand-independent nuclear localization of androgen receptor in refractory prostate cancer cells. The Prostate *67*, 509-520.

Sato, A., Asano, T., Ito, K., and Asano, T. (2012). Vorinostat and bortezomib synergistically cause ubiquitinated protein accumulation in prostate cancer cells. The Journal of urology *188*, 2410-2418.

Scher, H. I., Fizazi, K., Saad, F., Taplin, M. E., Sternberg, C. N., Miller, K., de Wit, R., Mulders, P., Chi, K. N., Shore, N. D.*, et al.* (2012). Increased survival with enzalutamide in prostate cancer after chemotherapy. The New England journal of medicine *367*, 1187-1197.

Siegel, R. L., Miller, K. D., and Jemal, A. (2015). Cancer statistics, 2015. CA: a cancer journal for clinicians *65*, 5-29.

Solit, D. B., Zheng, F. F., Drobnjak, M., Munster, P. N., Higgins, B., Verbel, D., Heller, G., Tong, W., Cordon-Cardo, C., Agus, D. B.*, et al.* (2002). 17-Allylamino-17-demethoxygeldanamycin induces the degradation of androgen receptor and HER-2/neu and inhibits the growth of prostate cancer xenografts. Clinical cancer research : an official journal of the American Association for Cancer Research *8*, 986-993.

Tam, W. L., and Weinberg, R. A. (2013). The epigenetics of epithelial-mesenchymal plasticity in cancer. Nature medicine *19*, 1438-1449.

Thakur, M. K., Heilbrun, L. K., Sheng, S., Stein, M., Liu, G., Antonarakis, E. S., Vaishampayan, U., Dzinic, S. H., Li, X., Freeman, S.*, et al.* (2015). A phase II trial of ganetespib,

a heat shock protein 90 Hsp90) inhibitor, in patients with docetaxel-pretreated metastatic castrate-resistant prostate cancer (CRPC)-a prostate cancer clinical trials consortium (PCCTC) study. Investigational new drugs.

Toren, P., Kim, S., Cordonnier, T., Crafter, C., Davies, B. R., Fazli, L., Gleave, M. E., and Zoubeidi, A. (2015). Combination AZD5363 with enzalutamide significantly delays enzalutamide-resistant prostate cancer in preclinical models. European urology *67*, 986-990.

Tran, C., Ouk, S., Clegg, N. J., Chen, Y., Watson, P. A., Arora, V., Wongvipat, J., Smith-Jones, P. M., Yoo, D., Kwon, A.*, et al.* (2009). Development of a second-generation antiandrogen for treatment of advanced prostate cancer. Science *324*, 787-790.

Uchida, H., Maruyama, T., Nishikawa-Uchida, S., Oda, H., Miyazaki, K., Yamasaki, A., and Yoshimura, Y. (2012). Studies using an in vitro model show evidence of involvement of epithelial-mesenchymal transition of human endometrial epithelial cells in human embryo implantation. The Journal of biological chemistry *287*, 4441-4450.

Veldscholte, J., Berrevoets, C. A., Zegers, N. D., van der Kwast, T. H., Grootegoed, J. A., and Mulder, E. (1992). Hormone-induced dissociation of the androgen receptor-heat-shock protein complex: use of a new monoclonal antibody to distinguish transformed from nontransformed receptors. Biochemistry *31*, 7422-7430.

Weichert, W., Roske, A., Gekeler, V., Beckers, T., Stephan, C., Jung, K., Fritzsche, F. R., Niesporek, S., Denkert, C., Dietel, M., and Kristiansen, G. (2008). Histone deacetylases 1, 2 and 3 are highly expressed in prostate cancer and HDAC2 expression is associated with shorter PSA relapse time after radical prostatectomy. British journal of cancer *98*, 604-610.

Welsbie, D. S., Xu, J., Chen, Y., Borsu, L., Scher, H. I., Rosen, N., and Sawyers, C. L. (2009). Histone deacetylases are required for androgen receptor function in hormone-sensitive and castrate-resistant prostate cancer. Cancer research *69*, 958-966.

Yuan, X., and Balk, S. P. (2009). Mechanisms mediating androgen receptor reactivation after castration. Paper presented at: Urologic Oncology: Seminars and Original Investigations (Elsevier).

Zegarra-Moro, O. L., Schmidt, L. J., Huang, H., and Tindall, D. J. (2002). Disruption of androgen receptor function inhibits proliferation of androgen-refractory prostate cancer cells. Cancer research *62*, 1008-1013.

Zhou, X., Yang, X. Y., and Popescu, N. C. (2010). Synergistic antineoplastic effect of DLC1 tumor suppressor protein and histone deacetylase inhibitor, suberoylanilide hydroxamic acid (SAHA), on prostate and liver cancer cells: perspectives for therapeutics. International journal of oncology *36*, 999-1005.

Zhou, X., Yang, X. Y., and Popescu, N. C. (2012). Preclinical evaluation of combined antineoplastic effect of DLC1 tumor suppressor protein and suberoylanilide hydroxamic acid on prostate cancer cells. Biochemical and biophysical research communications *420*, 325-330.

Molecular Pharmacology Fast Forward. Published on July 5, 2016 as DOI: 10.1124/mol.116.103416
This article has not been copyedited and formatted. The final version may differ from this version.

Footnotes

Financial Support Credit

This work was supported by a Department of Defense Prostate Cancer Research Program Idea Development Award to Zhihui Qin [W81XWH-12-1-0340], a Strategic Research Initiative Grant from Karmanos Cancer Institute to Zhihui Qin and Manohar Ratnam [KCI-2014-1] and a WSUSOM Cancer Biology Program NRSA-T32 Training Grant fellowship to Rayna Rosati [1T32 CA009531]. The study utilized the Wayne State University School of Medicine Pharmacology Core which is supported, in part, by NIH Center grant [P30 CA022453] to the Karmanos Cancer Institute at Wayne state University.

The new hybrid molecules reported in this manuscript are covered by U.S. Provisional Patent Application No. 62/288,810 filed by Wayne State University under the title "First-in-class Targeted Androgen Receptor Down-regulators (TARDs)".

Molecular Pharmacology Fast Forward. Published on July 5, 2016 as DOI: 10.1124/mol.116.103416
This article has not been copyedited and formatted. The final version may differ from this version.

Figure Legends

Figure 1. Compound structures and synthetic schemes. *Panel A*, Chemical structures of Enz, SAHA, **1005**, **2-75, 1002 and 3-52**. *Panel B*, Synthesis of **1005**, **2-75, 1002 and 3-52**. *Reagents and conditions*: (a) ethyl acrylate, $Pd(OAc)_2$, P(*o*-tolyl)$_3$, DIPEA, DMF, 80^{o}C, 75%; (b) 37% HCl (aq), acetonitrile, reflux, 91%; (c) NH_2OTHP, BOP, DIPEA, DMF, 51%; (d) HCl (4N in dioxane), MeOH, 60% for **1005**, 32% for **2-75**; (e) HCOOLi, Ac_2O, $Pd_2(dba)_3$, LiCl, DMF, 80^{o}C, 92%; (f) 7-amino-*N*-(tetrahydro-2*H*-pyran-2-yl)oxy heptanamide, HBTU, DIPEA, DMF, 30%; (g) methyl 7-aminoheptanoate hydrochloride, HBTU, DIPEA, DMF, 47%.

Figure 2. Measurement of intrinsic and *in situ* HDACi activities. *Panel A,* Dose-dependent inhibition of HDACs from Hela cell nuclear extract by **2-75**, **1005** and **SAHA**. Hela cell nuclear extract was incubated with each drug at the indicated concentrations. IC_{50} values were calculated from nonlinear regression plots using GraphPad Prism5 software. *Panel B,* Enz, **1002** and **3-52** were tested against HeLa cell nuclear extract at 10 μM and 25 μM and TSA (1μM) was used as positive control. *Panel C,* Dose-dependent inhibition of recombinant HDAC6 by **2-75**, **1005** and **SAHA**. Recombinant HDAC6 was incubated with each drug at the indicated concentrations. IC_{50} values were calculated from nonlinear regression plots using GraphPad Prism5 software. *Panel D,* Enz, **1002** and **3-52** were tested against recombinant HDAC6 at 10 μM and 25 μM and TSA (1μM) was used as positive control. *Panel E,* LNCaP cells were treated with the indicated compounds (10 μM) or vehicle (DMSO) for 48h. Cells were then harvested to quantify mRNA for DLC1 and values were normalized to the values for GAPDH mRNA. *Panel F,* C4-2 cells were treated with the indicated concentrations of Enz, SAHA, **2-75** or **1005** or vehicle (DMSO) for 48h. Cells were then harvested to quantify mRNA for DLC1 and values were

Molecular Pharmacology Fast Forward. Published on July 5, 2016 as DOI: 10.1124/mol.116.103416
This article has not been copyedited and formatted. The final version may differ from this version.

normalized to the values for GAPDH mRNA. In all panels, the error bars represent standard deviation of experimental triplicates. Where indicated, $P < 0.05$

Figure 3: Testing the ability of compounds to interact with AR and to induce chromatin association of AR. *Panels A and B* show data obtained using C4-2 cells. After 96h of hormone depletion cells were treated with R1881 (1nM) and 1 μM , 2.5 μM , 5 μM , 10 μM of the indicated compound or vehicle (DMSO) for 48h. Cells were then harvested to purify total RNA. The mRNAs for KLK3 and TMPRSS2 were quantified by normalizing to the values for GAPDH mRNA. In all panels, the error bars represent standard deviation of experimental triplicates. In *Panel C,* C4-2 cells plated in hormone-depleted medium were treated with either vehicle, R1881, or the indicated compound for 2h. Cells were harvested and subjected to ChIP using AR antibody. Taqman probes targeting ARE enhancer elements associated with the KLK3 gene were used to quantify the immunoprecipitated chromatin. In all panels, the error bars represent standard deviation of experimental triplicates. $p<0.01$

Figure 4: Modulation of protein levels and hyper-acetylation. C4-2 cells were treated with the indicated concentrations of Enz, SAHA, **1005** or **2-75** or with vehicle (DMSO) for time indicated. Cells were then harvested for western blot analysis using antibody to AR *(Panel A)*, HSP90 *(Panel B*), Acetyl-Lysine (*Panel C*) or GAPDH (loading control). ImageJ software was used to determine the intensities of the bands relative to the vehicle control for each protein. The values were then divided by the values for GAPDH within the same samples.

Figure 5: Induction of AR degradation.C4-2 cells were pre-treated with cycloheximide (CHX, 20 μM) or with vehicle for 2 h followed by the introduction of Enz (10 μM), SAHA (10 μM), **1005** (10 μM) or **2-75** (10 μM) or vehicle for the indicated durations. Cells were then harvested for western blot analysis and probed with antibody to AR, p21, or α tubulin (loading control).

Molecular Pharmacology Fast Forward. Published on July 5, 2016 as DOI: 10.1124/mol.116.103416
This article has not been copyedited and formatted. The final version may differ from this version.

ImageJ software was used to determine the intensities of the bands relative to the zero hour time point for each treatment.

Figure 6: Hyper-acetylation of α-tubulin and histones H3 and H4. C4-2 cells were treated with Enz, SAHA, **1005** or **2-75** (2.5 μM, 5 μM, 10 μM) or vehicle for 24h. Cells were then harvested for western blot analysis and probed with antibody to acetyl-histone H3, acetyl-histone H4, acetyl-tubulin, or α-tubulin. ImageJ software was used to determine the intensities of the bands of acetyl-tubulin relative to the total amount of tubulin for each treatment. The ratio of acetyl-tubulin to total tubulin in each sample is indicated.

Figure 7: Induction of p21 mRNA. *Panel A*, LNCaP cells were treated with Enz, SAHA, **1005** or **2-75** at a concentration of 10 μM or with vehicle (DMSO) for 48h. Cells were then harvested to quantify p21 mRNA and the values were normalized to those for GAPDH mRNA. Panel B, C4-2 cells were treated with Enz, SAHA, **1005** or **2-75** at the indicated concentrations or with vehicle (DMSO) for 48h. Cells were then harvested to quantify p21 mRNA and the values were normalized to those for GAPDH mRNA. *Panel C*. C4-2 cells were treated with either Enz (10 μM) or SAHA (10 μM), an equimolar (10 μM each) mixture of Enz and SAHA, **2-75** (10 μM) or **1005** (10 μM) Cells were then harvested to quantify p21 mRNA and the values were normalized to those for GAPDH mRNA. In all panels, the error bars represent standard deviation of experimental triplicates. Where indicated, $P < 0.05$

Figure 8: Effects on cell viability in Enz-resistant CRPC cells. In *Panel A,* C4-2 cells were seeded in 96-well plates and 24h later, they were treated with the indicated compounds (2.5 uM, 5 uM or 10 uM) or with vehicle (DMSO). Cell density was measured by the MTT assay on Days 0 and 3 of treatment. Values equal to or above that on Day 0 were considered to represent 100 percent viability. In *Panel B*, C4-2 cells were seeded and treated 24h later with Enz (2.5 uM),

Molecular Pharmacology Fast Forward. Published on July 5, 2016 as DOI: 10.1124/mol.116.103416
This article has not been copyedited and formatted. The final version may differ from this version.

SAHA (2.5 uM), an equimolar mixture of Enz and SAHA (each compound at 2.5 uM), **2-75** (2.5 uM), **1005** (2.5 uM), or with vehicle (DMSO). Cell density was measured by the MTT assay on Days 0 and 3 of treatment. The Y-axis shows percent cell growth on Day 3 relative to the cell density on Day 0. In *Panel C*, PC3 cells were seeded in 96-well plates and 24h later, they were treated with the indicated compounds (2.5 uM, 5 uM or 10 uM) or with vehicle (DMSO). Cell density was measured by the MTT assay on Days 0 and 3 of treatment. Values equal to or above that on Day 0 were considered to represent 100 percent viability. In all panels, the error bars represent standard deviation of experimental sextuplicate samples. Where indicated, $P < 0.05$

Figure 9: Mechanistic model for the actions of compounds 1005 and 2-75. In the absence of bound ligand AR is in a stable complex with HSP90 which is maintained in a hypo-acetylated state by HDAC6 (Panel A). Hypo-acetylated HSP90 stabilizes AR and also supports cell survival through regulation of its other client proteins. When **2-75** or **1005** bind to AR in the chaperone complex their HDACi moieties inhibit HDAC6 that associates with the complex. Despite their relatively weak intrinsic HDACi activities, the efficiency of HDAC6 inhibition by the hybrid molecules is enhanced by their localized effect in the chaperone complex. This results in hyper-acetylation of HSP90 leading to destabilization of AR and also loss of cell survival through deregulation of other HSP90 client proteins (Panel B).

Figure 1

A.

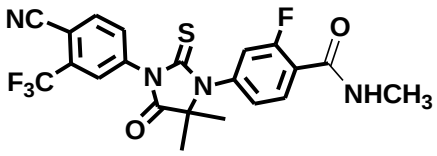

Enzalutamide

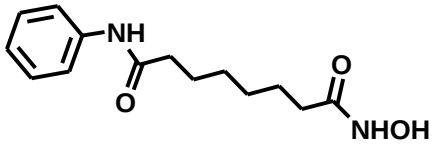

SAHA

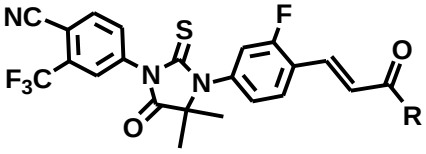

R= NHOH, Compoud 1005;
R= OEt, Compound 1002

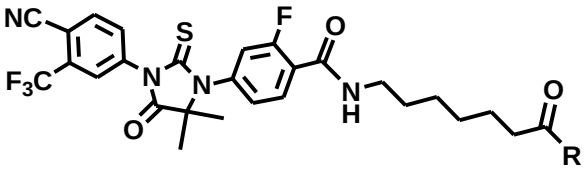

R=NHOH, Compound 2-75;
R=OMe, Compound 3-52

B.

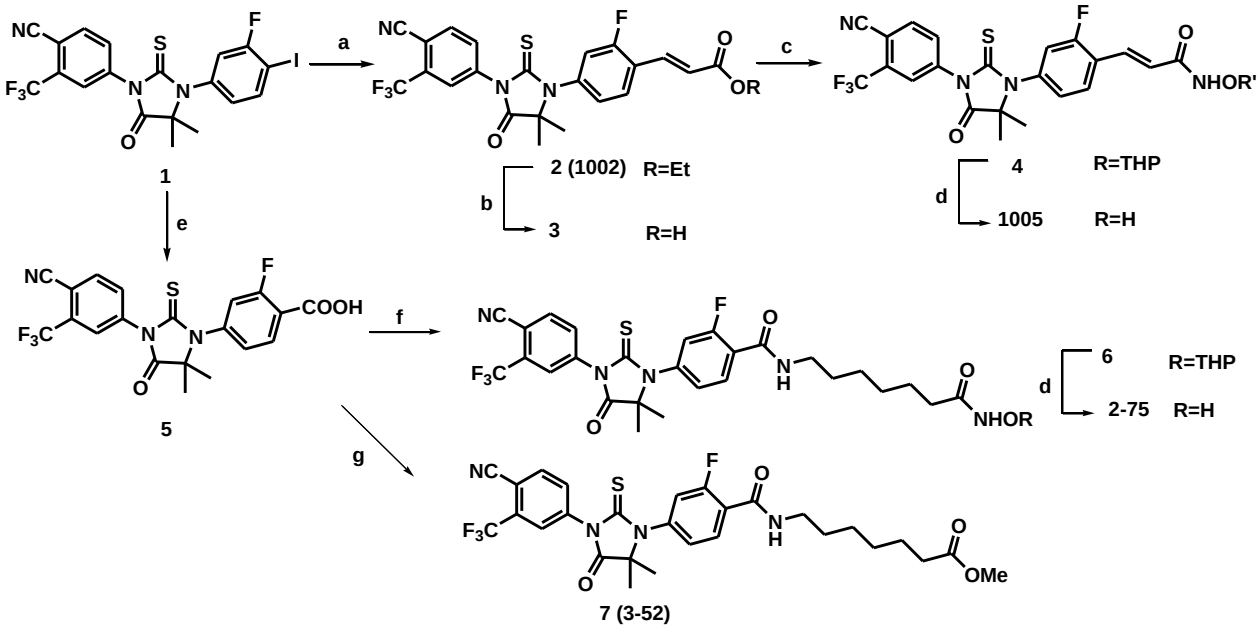

Figure 2

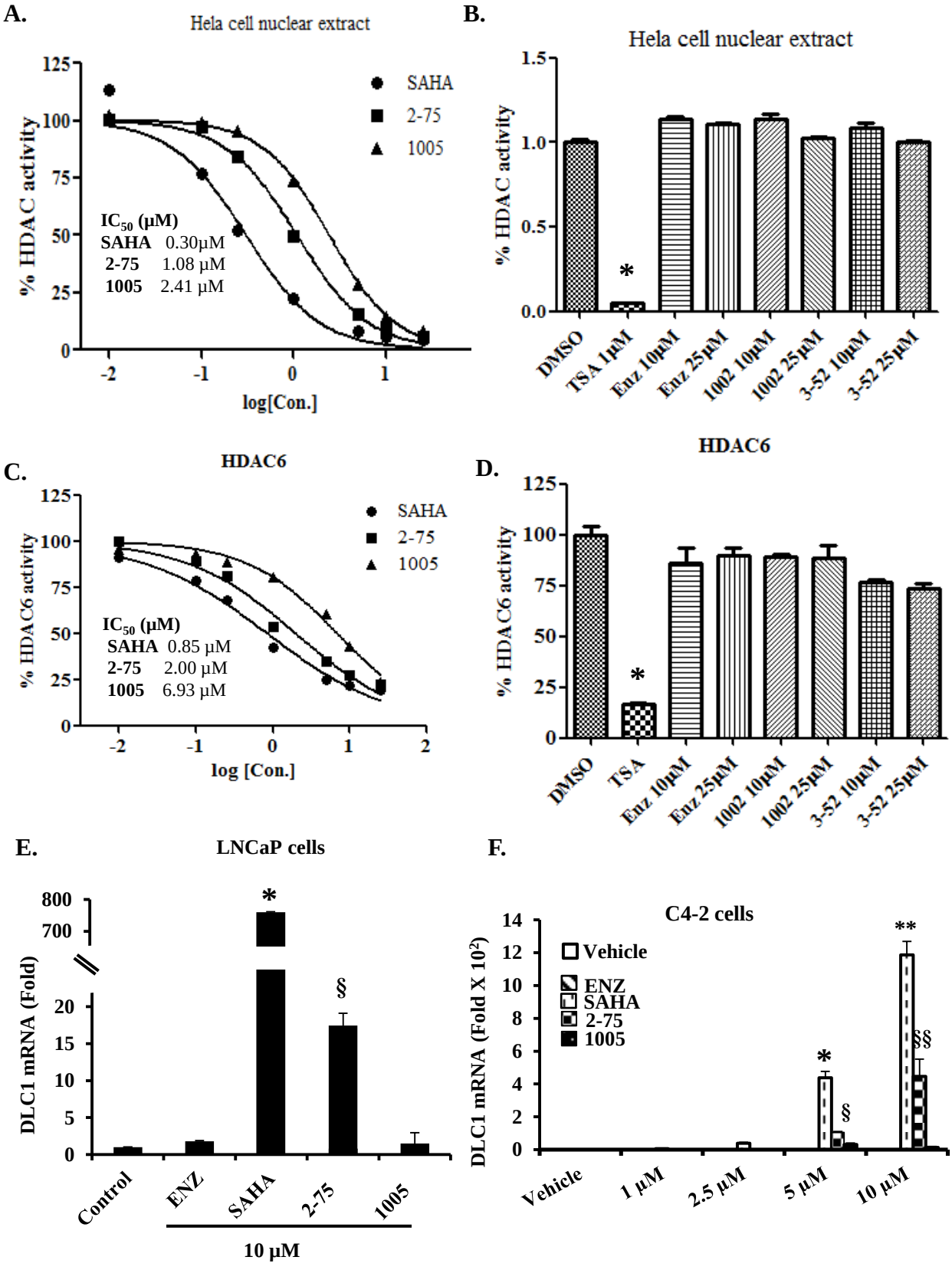
A.
Hela cell nuclear extract
% HDAC activity
log[Con.]
SAHA
2-75
1005
IC50 (μM)
SAHA 0.30μM
2-75 1.08 μM
1005 2.41 μM
B.
Hela cell nuclear extract
% HDAC activity
DMSO
TSA 1μM
Enz 10μM
Enz 25μM
1002 10μM
1002 25μM
3-52 10μM
3-52 25μM
C.
HDAC6
% HDAC6 activity
log [Con.]
SAHA
2-75
1005
IC50 (μM)
SAHA 0.85 μM
2-75 2.00 μM
1005 6.93 μM
D.
HDAC6
% HDAC6 activity
DMSO
TSA
Enz 10μM
Enz 25μM
1002 10μM
1002 25μM
3-52 10μM
3-52 25μM
E.
LNCaP cells
DLC1 mRNA (Fold)
Control
ENZ
SAHA
2-75
1005
10 μM
F.
C4-2 cells
DLC1 mRNA (Fold X 10²)
Vehicle
ENZ
SAHA
2-75
1005
Vehicle
1 μM
2.5 μM
5 μM
10 μM

Figure 3

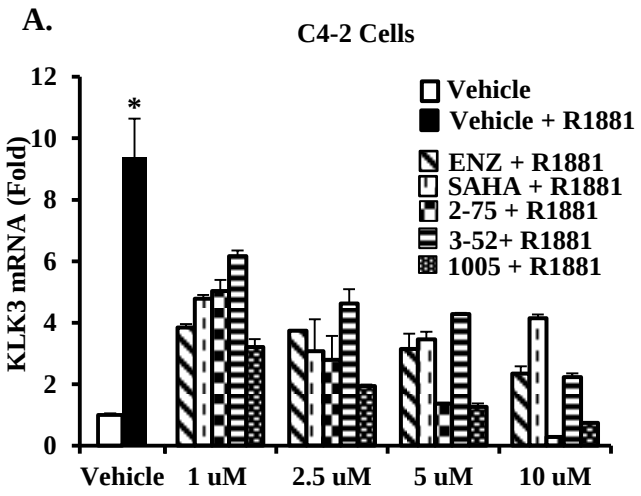
A.
C4-2 Cells
KLK3 mRNA (Fold)
12
10
8
6
4
2
0
*
Vehicle
Vehicle + R1881
ENZ + R1881
SAHA + R1881
2-75 + R1881
3-52+ R1881
1005 + R1881
Vehicle
1 uM
2.5 uM
5 uM
10 uM

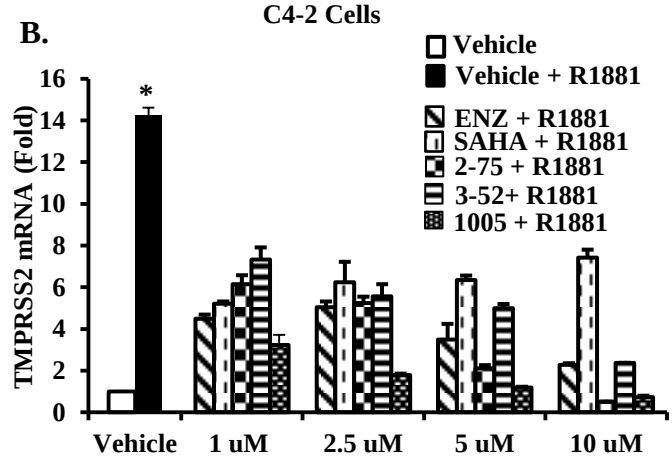
B.
C4-2 Cells
TMPRSS2 mRNA (Fold)
16
14
12
10
8
6
4
2
0
*
Vehicle
Vehicle + R1881
ENZ + R1881
SAHA + R1881
2-75 + R1881
3-52+ R1881
1005 + R1881
Vehicle
1 uM
2.5 uM
5 uM
10 uM

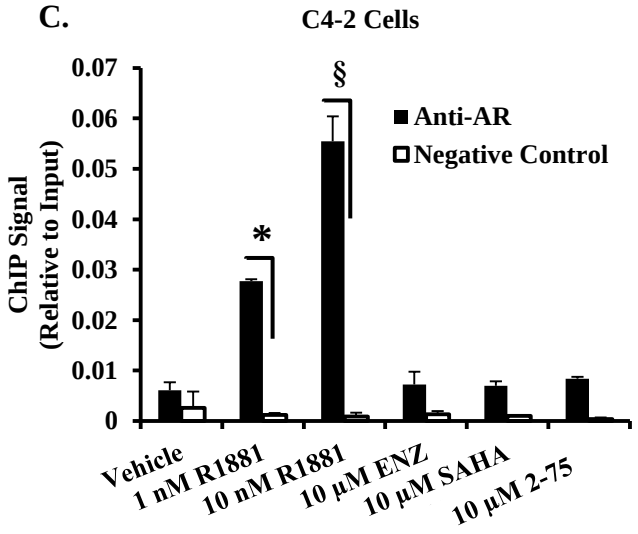
C.
C4-2 Cells
ChIP Signal
(Relative to Input)
0.07
0.06
0.05
0.04
0.03
0.02
0.01
0
*
§
Anti-AR
Negative Control
Vehicle
1 nM R1881
10 nM R1881
10 μM ENZ
10 μM SAHA
10 μM 2-75

Figure 4

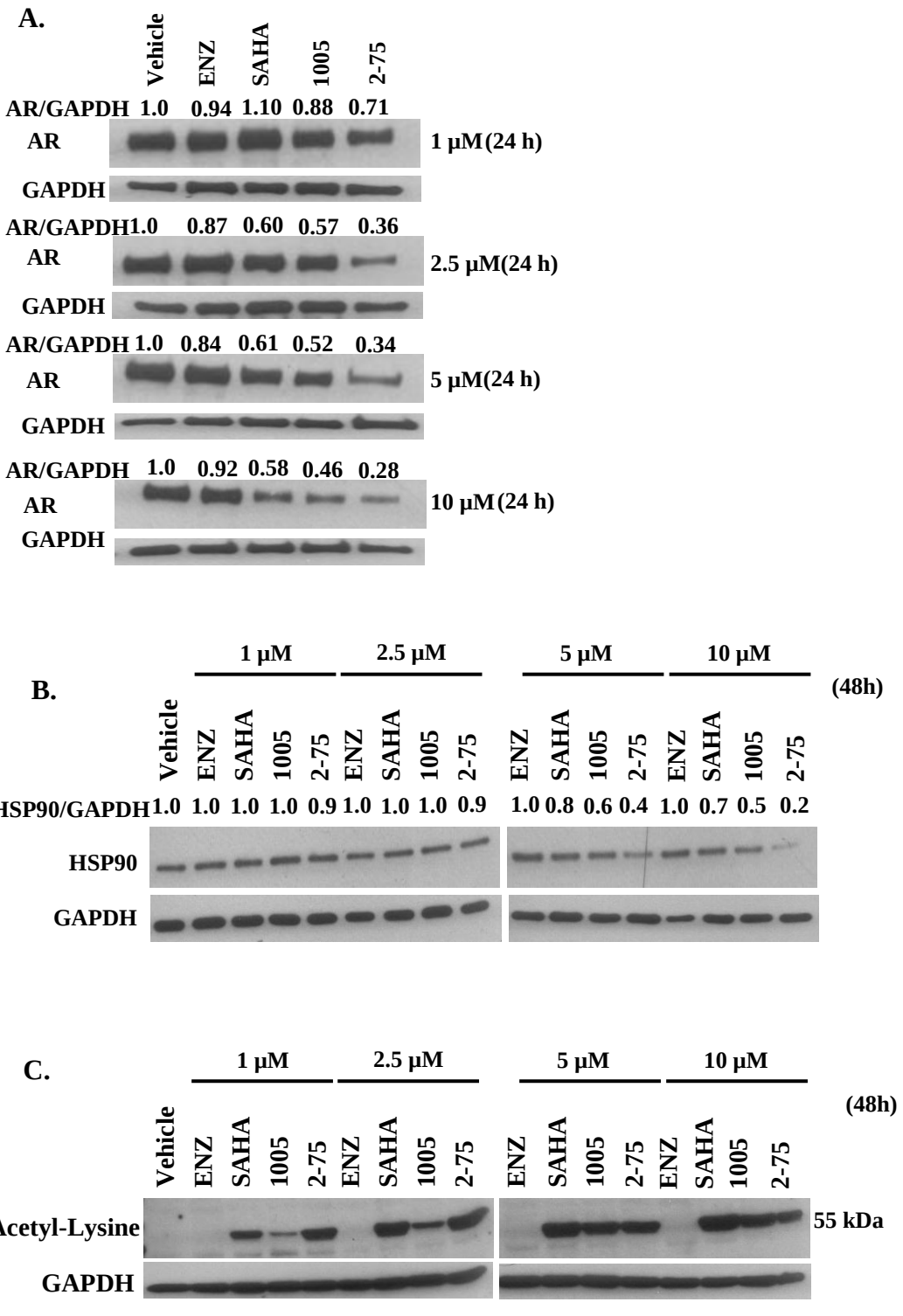
A.
Vehicle
ENZ
SAHA
1005
2-75
AR/GAPDH 1.0 0.94 1.10 0.88 0.71
AR
1 μM (24 h)
GAPDH
AR/GAPDH 1.0 0.87 0.60 0.57 0.36
AR
2.5 μM (24 h)
GAPDH
AR/GAPDH 1.0 0.84 0.61 0.52 0.34
AR
5 μM (24 h)
GAPDH
AR/GAPDH 1.0 0.92 0.58 0.46 0.28
AR
10 μM (24 h)
GAPDH
B.
1 μM
2.5 μM
5 μM
10 μM
(48h)
Vehicle
ENZ
SAHA
1005
2-75
HSP90/GAPDH 1.0 1.0 1.0 1.0 0.9 1.0 1.0 1.0 0.9 1.0 0.8 0.6 0.4 1.0 0.7 0.5 0.2
HSP90
GAPDH
C.
1 μM
2.5 μM
5 μM
10 μM
(48h)
Vehicle
ENZ
SAHA
1005
2-75
Acetyl-Lysine
55 kDa
GAPDH

Figure 5

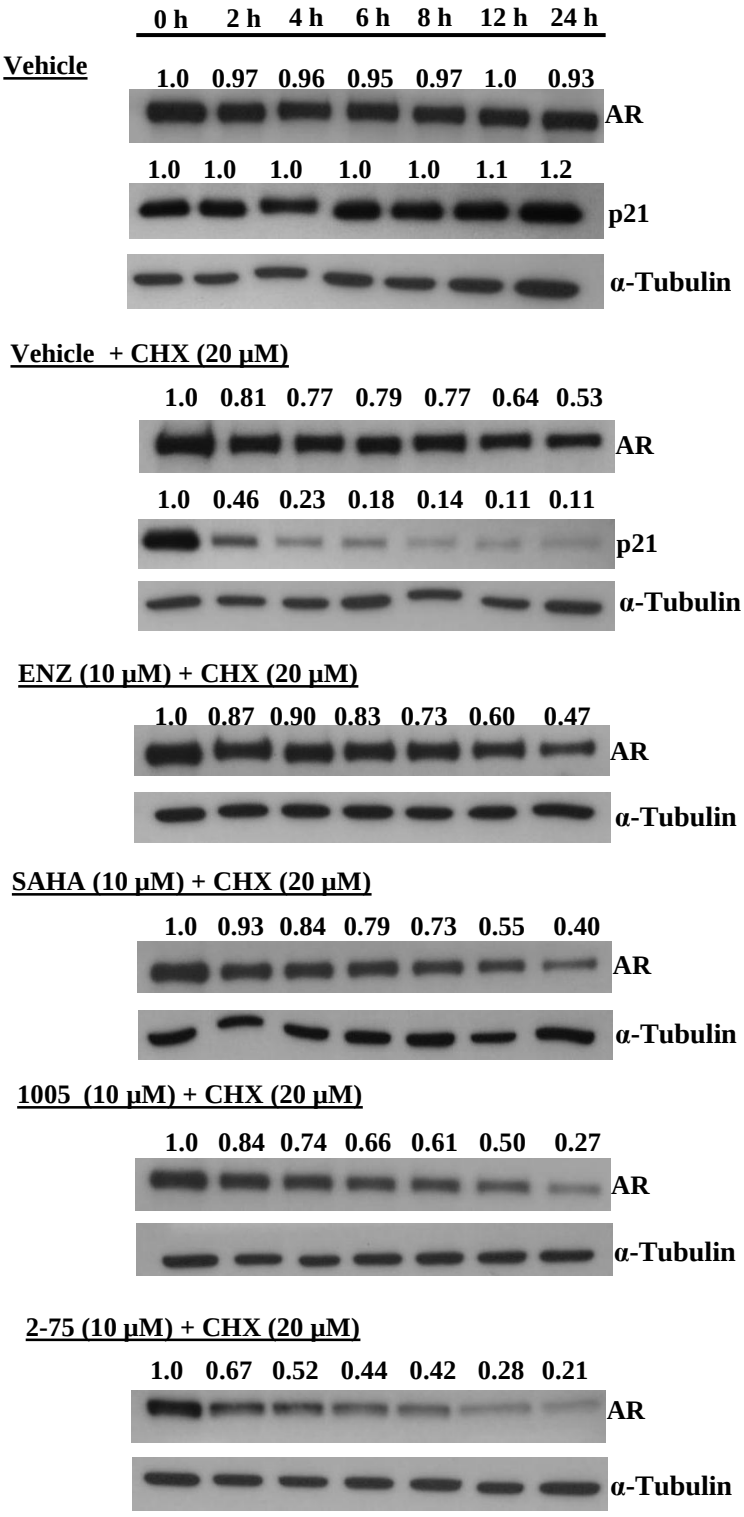
0 h 2 h 4 h 6 h 8 h 12 h 24 h
Vehicle
1.0 0.97 0.96 0.95 0.97 1.0 0.93
AR
1.0 1.0 1.0 1.0 1.0 1.1 1.2
p21
α-Tubulin
Vehicle + CHX (20 μM)
1.0 0.81 0.77 0.79 0.77 0.64 0.53
AR
1.0 0.46 0.23 0.18 0.14 0.11 0.11
p21
α-Tubulin
ENZ (10 μM) + CHX (20 μM)
1.0 0.87 0.90 0.83 0.73 0.60 0.47
AR
α-Tubulin
SAHA (10 μM) + CHX (20 μM)
1.0 0.93 0.84 0.79 0.73 0.55 0.40
AR
α-Tubulin
1005 (10 μM) + CHX (20 μM)
1.0 0.84 0.74 0.66 0.61 0.50 0.27
AR
α-Tubulin
2-75 (10 μM) + CHX (20 μM)
1.0 0.67 0.52 0.44 0.42 0.28 0.21
AR
α-Tubulin

Figure 6

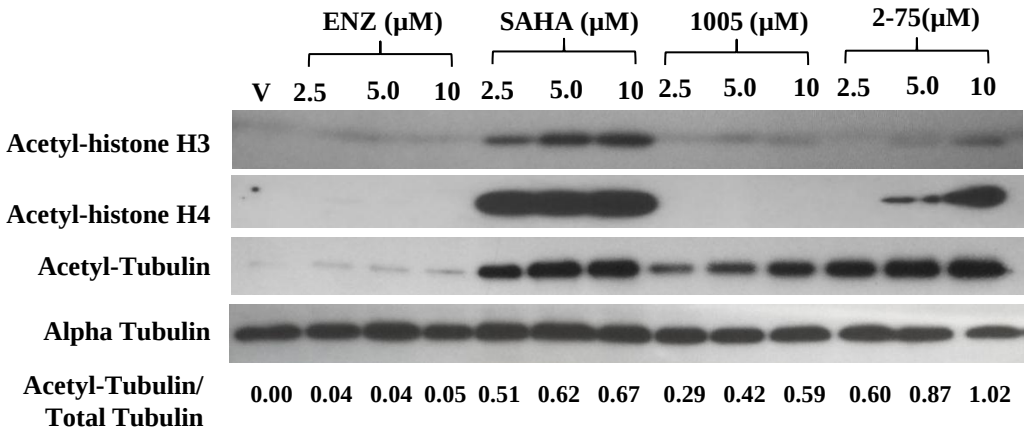
ENZ (μM)
SAHA (μM)
1005 (μM)
2-75(μM)
V 2.5 5.0 10 2.5 5.0 10 2.5 5.0 10 2.5 5.0 10
Acetyl-histone H3
Acetyl-histone H4
Acetyl-Tubulin
Alpha Tubulin
Acetyl-Tubulin/ Total Tubulin
0.00 0.04 0.04 0.05 0.51 0.62 0.67 0.29 0.42 0.59 0.60 0.87 1.02

Figure 7

A.

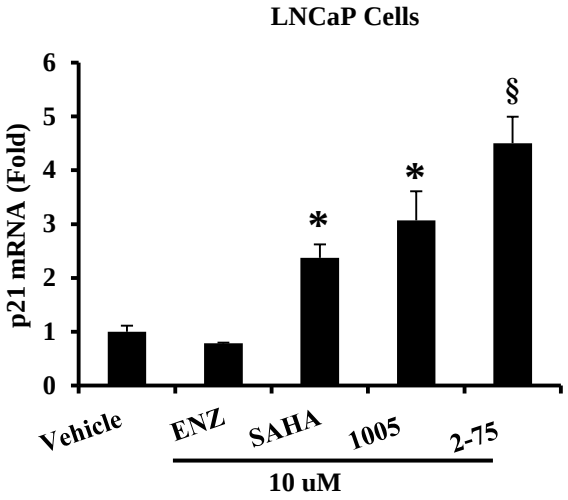

B.

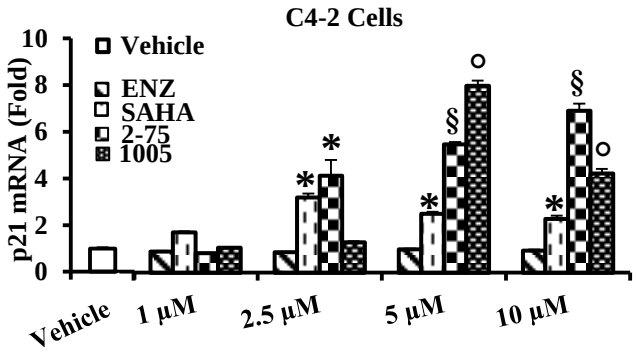

C.

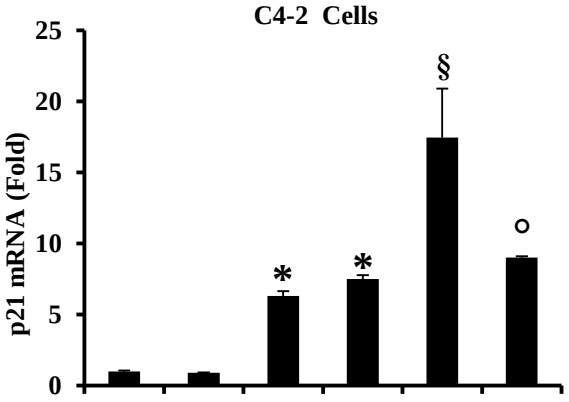

Vehicle	+	-	-	-	-	-
ENZ (10 µM)	-	+	-	+	-	-
SAHA (10 µM)	-	-	+	+	-	-
2-75 (10 µM)	-	-	-	-	+	-
1005 (10 µM)	-	-	-	-	-	+

Figure 8

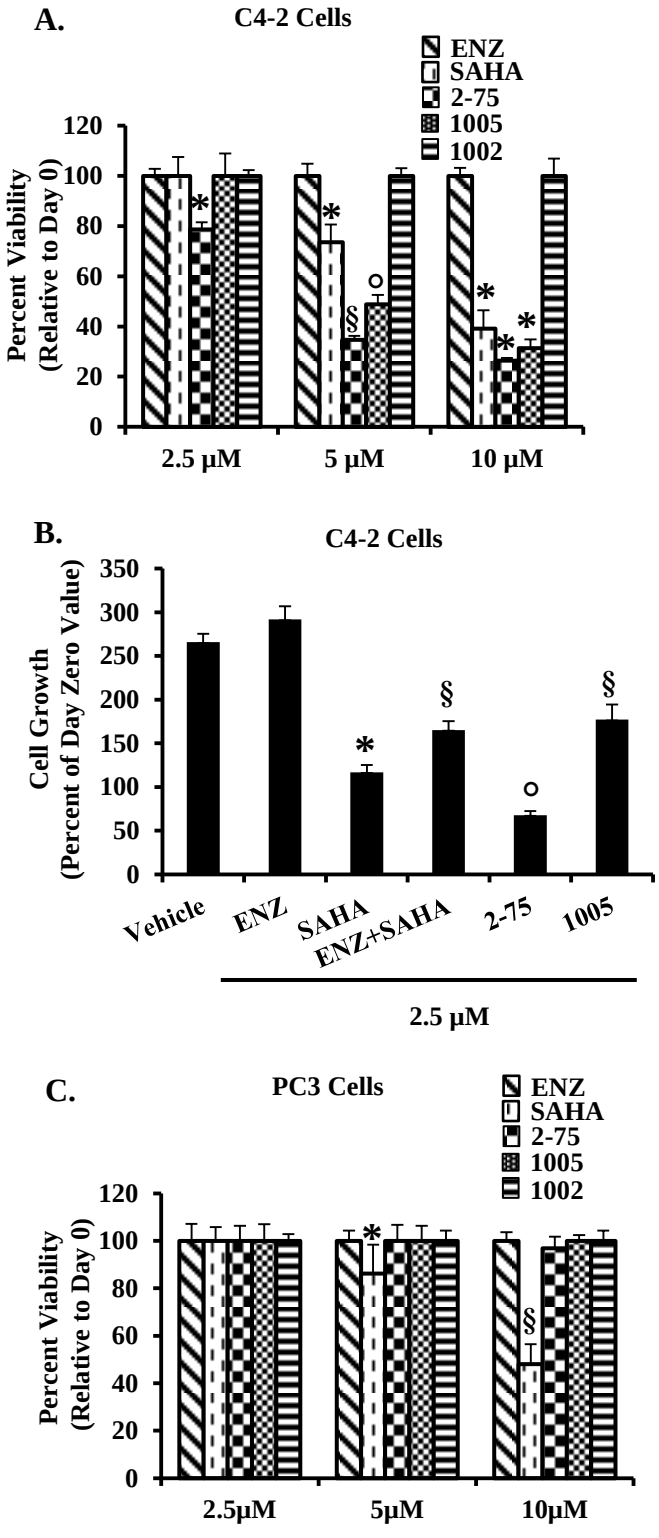
A.
C4-2 Cells
ENZ
SAHA
2-75
1005
1002
Percent Viability
(Relative to Day 0)
120
100
80
60
40
20
0
2.5 µM
5 µM
10 µM
B.
C4-2 Cells
Cell Growth
(Percent of Day Zero Value)
350
300
250
200
150
100
50
0
Vehicle
ENZ
SAHA
ENZ+SAHA
2-75
1005
2.5 µM
C.
PC3 Cells
ENZ
SAHA
2-75
1005
1002
Percent Viability
(Relative to Day 0)
120
100
80
60
40
20
0
2.5µM
5µM
10µM

Figure 9

A.

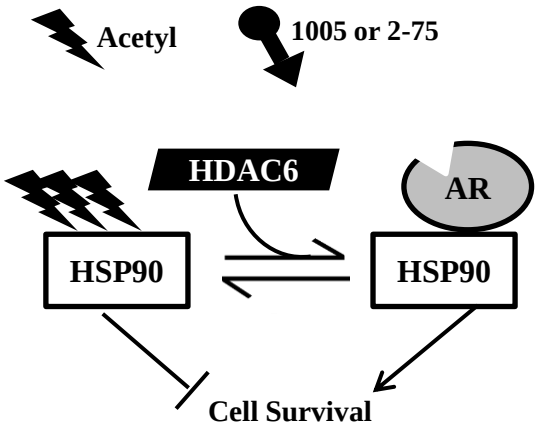
Acetyl
1005 or 2-75
HDAC6
AR
HSP90
HSP90
Cell Survival

B.

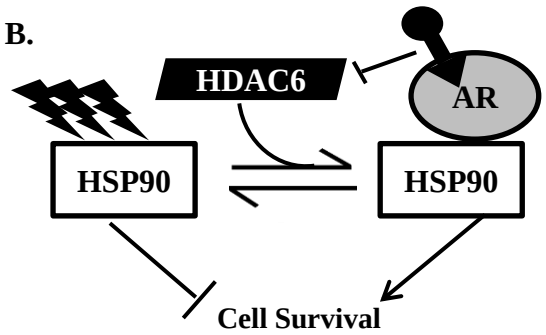
HDAC6
AR
HSP90
HSP90
Cell Survival